

Reliability checks on the Indo-US Stellar Spectral Library using Artificial Neural Networks and Principal Component Analysis

Harinder P. SINGH

Department of Physics & Astrophysics, University of Delhi, Delhi - 110007, India

hpsingh@physics.du.ac.in

Manabu YUASA and Nawo YAMAMOTO

Research Institute for Science & Technology, Kinki University, Higashi-Osaka, Osaka 577-8502, Japan

yuasa@rist.kindai.ac.jp

and

Ranjan GUPTA

Inter-University Center for Astronomy & Astrophysics, Ganeshkhind, Pune- 411007, India

rag@iucaa.ernet.in

(Received ; accepted)

Abstract

The Indo-US coude feed stellar spectral library (CFLIB) made available to the astronomical community recently by Valdes et al. (2004) contains spectra of 1273 stars in the spectral region 3460 to 9464 Å at a high resolution of 1 Å FWHM and a wide range of spectral types. Cross-checking the reliability of this database is an important and desirable exercise since a number of stars in this database have no known spectral types and a considerable fraction of stars has not so complete coverage in the full wavelength region of 3460-9464 Å resulting in gaps ranging from a few Å to several tens of Å. In this paper, we use an automated classification scheme based on Artificial Neural Networks (ANN) to classify all 1273 stars in the database. In addition, principal component analysis (PCA) is carried out to reduce the dimensionality of the data set before the spectra are classified by the ANN. Most importantly, we have successfully demonstrated employment of a variation of the PCA technique to restore the missing data in a sample of 300 stars out of the CFLIB.

Key words: Stars: general – Methods: data analysis – Catalogs

1. Introduction

Automated schemes of data validation and analysis have assumed added significance recently as larger databases are increasingly becoming available in almost all areas of observational astronomy. With the advent of bigger CCD detectors in spectroscopy, the need for having large libraries of stellar spectra at high spectral resolution is also getting fulfilled. Jacoby, Hunter, & Christian (1984, hereafter JHC) made 158 spectra available in the range of 3510-7427Å at 4.5Å resolution. Prugniel & Soubiran (2001) published a library of 708 stars using the ELODIE échelle spectrograph at the Observatoire de Haute-Provence that covers a wavelength band of 4100-6800 Å at a resolution of $R=42,000$. Cenarro et al. (2001) have provided a database of 706 stellar spectra in the wavelength region 8350-9020 Å at 1.5 Å resolution and Le Borgne et al. (2003, hereafter STELIB) with 247 spectra in the range of 3200-9500Å at 3Å resolution. Moulataka et.al. (2004, hereafter ELODIE) compiled 1959 spectra in the range of 4000-6800Å at a resolution of 0.55Å .

More recently, Valdes et al. (2004) observed more than 1200 stars with emphasis on broad wavelength coverage (3400-9500 Å) at a resolution of ~ 1 Å FWHM at an original dispersion of 0.44 Å per pixel. Their coude feed stellar spectral library (CFLIB) provides a resolution sufficient to resolve numerous diagnostic spectral features that can be used in the automated parameterization of spectra.

Neural networks are a form of multiprocessor computing system, with simple processing elements with a high degree of inter-connection, simple scalar messaging and adaptive interaction between elements. In a supervised back propagation algorithm, the network topology is constrained to be feed-forward, i.e., connections are generally allowed from the input layer to the first (and mostly only) hidden layer; from the first hidden layer to the second,..., and from the last hidden layer to the output layer. The hidden layer learns to recode (or to provide a representation for) the inputs. More than one hidden layer can be used. The architecture is more powerful than single-layer networks: it can be shown that any mapping can be learned, given two hidden layers (of units).

Automated schemes like the Artificial Neural Networks (ANN) have been used in Astronomy for a number of data analysis tasks like scheduling observations (Johnson and Adorf, 1992), adaptive optics (Angel, Wizinowich and Lloyd-Hart, 1990), stellar spectral classification (Gulati et al., 1994; von Hippel et al. 1994) and star-galaxy separation studies (Odewahn et al., 1992). In addition Gulati, Gupta and Rao (1997) extended the ANN analysis to compare synthetic and observed spectra of G and K dwarfs. Gulati, Gupta and Singh (1997) estimated interstellar extinction $E(B-V)$ using ANN from low-dispersion ultraviolet spectra for O and B stars. Bailer-Jones, Gupta and Singh (2002) provide a review of the ANN applications in astronomical spectroscopy.

Another powerful statistical tool for data analysis is the Principal component analysis

Table 1. ANN training and test cases. Two hidden layers were used for all the cases

Case	Training (Library, No. of Spectra)	Testing (Library, No. of Spectra)	λ Region (used)	Resolution	Class. error
A1	JHC, 158	CFLIB, 1273	4100-5500Å	4.5Å	674.3
A2	JHC, 158	ELODIE, 1959	4100-5500Å	4.5Å	514.8
A3	JHC, 158	STELIB, 247	3600-7400Å	4.5Å	861.2
B1	ELODIE, 174	ELODIE, 1959	4000-5500Å	1Å	496.4
B2	ELODIE, 174	ELODIE, 1959	4000-6800Å	1Å	576.0
B3	ELODIE, 174	CFLIB, 1272	4000-5500Å	1Å	742.7
B4	ELODIE, 174	CFLIB, 1273	4000-6800Å	1Å	848.5
C1	STELIB, 247	CFLIB, 1273	4000-6800Å	3Å	643.9
C2	STELIB, 247	CFLIB, 1273	3500-9400Å	3Å	670.6
C3	STELIB, 247	ELODIE, 1959	4000-6800Å	3Å	501.8

(PCA). It involves a mathematical procedure that transforms a number of (possibly) correlated variables into a (smaller) number of uncorrelated variables called principal components. The first principal component accounts for as much of the variability in the data as possible, and each succeeding component accounts for as much of the remaining variability as possible. Objectives of principal component analysis are to discover or to reduce the dimensionality of a data set and to identify new meaningful underlying variables. The technique has been used widely for a number of applications in Astronomy, viz., for stellar classification by Murtagh and Heck (1987), Storrie-Lombardi et al. (1994) and Singh et al. (1998), by Francis et al. (1992) for QSO spectra, and for galaxy spectra by Sodr e and Cuevas (1994), Connolly et al. (1995), Lahav et al. (1996) and Folkes, Lahav and Maddox (1996).

Another important application was developed by Unno and Yuasa (1992, 2000) for supplementing missing observational data using a generalized PCA technique. Subsequently, Yuasa, Unno and Magono (1999) made use of this technique to determine distances of 183 mass-losing red giants.

The primary aim of this paper is to perform validity checks on the CFLIB by running the ANN code on various inter library sets like JHC, ELODIE and STELIB. In the next section we describe the ANN analysis. In Section 3, we demonstrate the possibility of using PCA for filling the gaps in the spectra of CFLIB. In Section 4, we summarize important conclusions of the study.

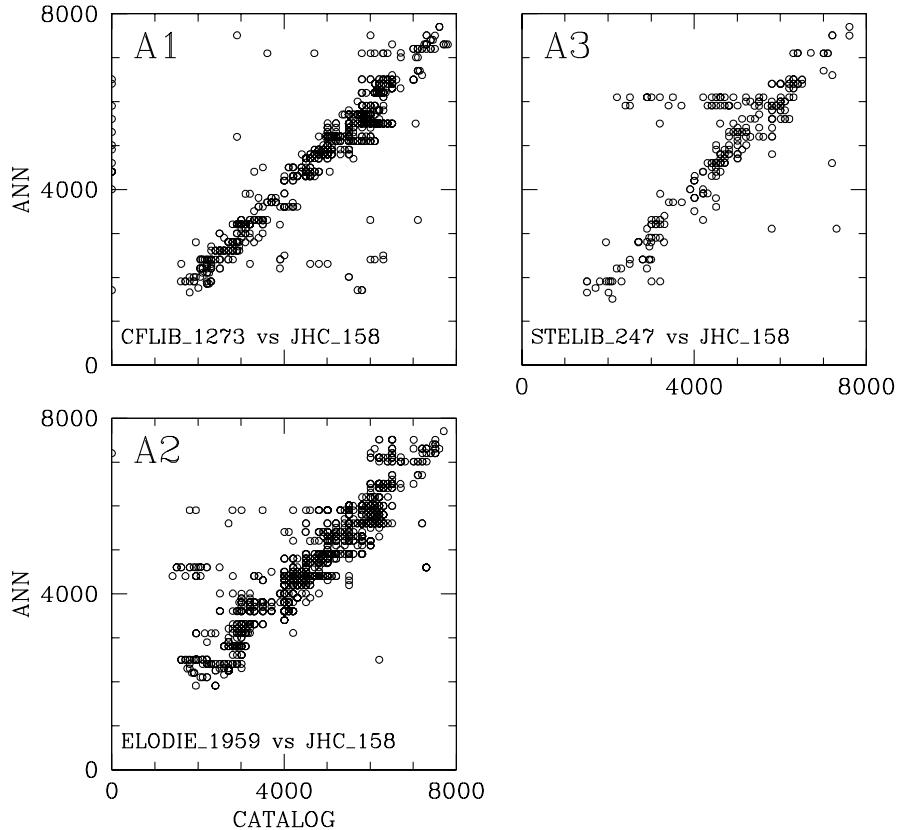


Fig. 1. Classification scatter plots for Cases A1-A3

2. ANN Analysis

A classification scheme using ANN involves two stages. A training stage and a testing stage. In the training stage, the input patterns and the desired output patterns are defined before the learning process of the ANN is carried out. During training, the network output and the desired output are compared and the network weights are adjusted. We employ a back propagation algorithm (Rumelhart, Hinton and Williams, 1986) to achieve this. The learning is stopped when the desired error threshold is reached and the network weights are frozen for use with the test set. In the testing stage, the test patterns are used by the network and classified in terms of the training classes.

In what follows, we have trained the ANN on three libraries with a view to run validity checks on the CFLIB. Three libraries that we used for training are:

1. JHC (Jacoby, Hunter and Christian, 1984) with 158 spectra available in the range of 3510-7427Å at 4.5Å resolution
2. ELODIE (Moultaka et al., 2004) with 1959 spectra in the range of 4000-6800Å at a resolution of 0.55Å

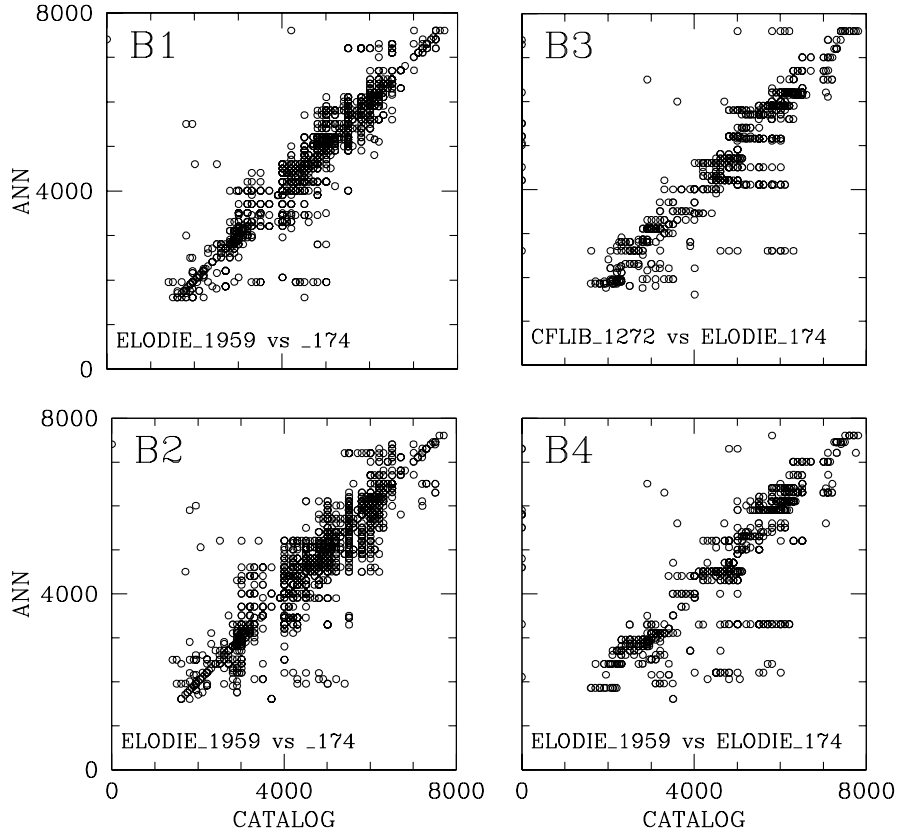


Fig. 2. Classification scatter plots for Case B1-B4

3. STELIB (Le Borgne et al., 2003) with 247 spectra in the range of 3200-9500Å at 3Å resolution

A total of 10 test cases were run and are summarized in Table 1. We also give the wavelength region used in each case, resolution and the resulting classification error. Cases A1-A3 involved training of the ANN by JHC and testing on, respectively, the CFLIB, ELODIE, and STELIB. Cases B1-B4 involved training the ANN with 174 individual classes of ELODIE and testing on ELODIE (4000-5500 Å , Case B1), ELODIE (4000-6800 Å , Case B2), CFLIB (4000-5500 Å , Case B3), and CFLIB (4000-6800 Å , Case B4). The last three cases C1-C3 involved training on STELIB and testing on CFLIB (4000-6800 Å , Case C1), CFLIB (3500-9400 Å , Case C2), and ELODIE (4000-6800 Å , Case C3).

The resolution used for training and testing for cases A1-A3 is 4.5 Å which is the resolution of JHC, 1 Å for cases B1-B4 which is the resolution of CFLIB, and 3 Å for cases C1-C3 which is the resolution of STELIB. The higher resolutions of some of the testing cases were degraded to match the resolution of the training library by gaussian convolution. The testing is done on the complete libraries, i.e., for 247 stars of STELIB, 1959 stars of ELODIE,

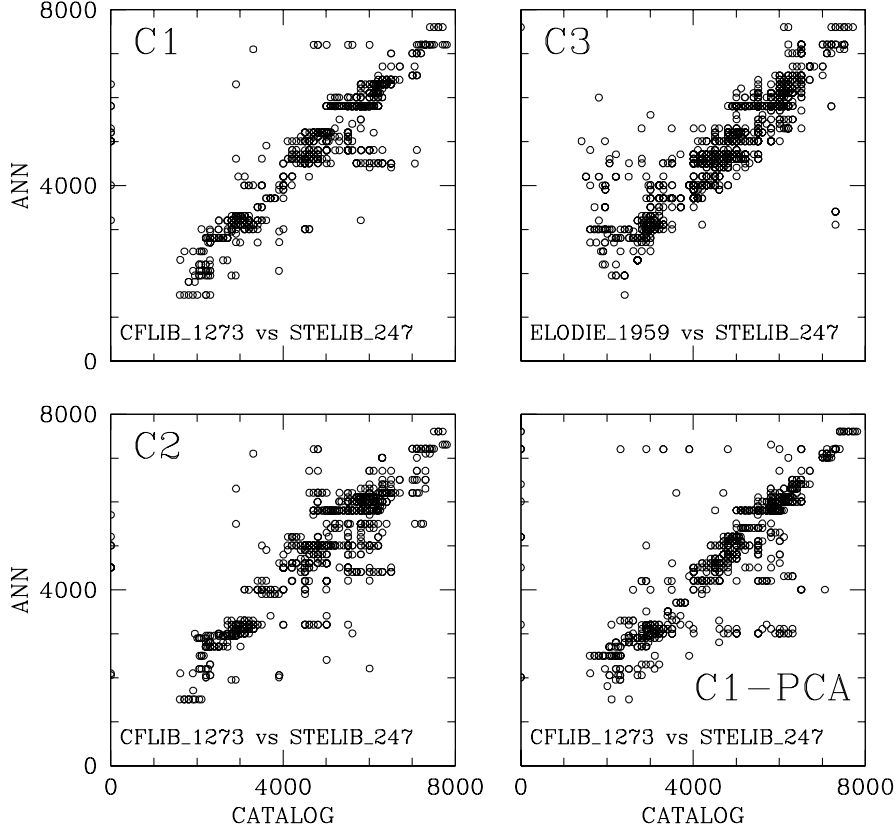


Fig. 3. Classification scatter plots for Case C1-C3. Also shown is case C1 with PCA preprocessing where first 15 principal components were used

and 1273 stars of CFLIB.

The classification scatter plots from these analysis are shown in Figures 1-3. The MK spectral types have been coded numerically for use by the ANN. The MK alphabetic class O is given a numeric code of 1000, B is 2000, A is 3000, and so on with M being 7000. The subclasses are multiplied by 100 and added in, thus a F5 star is coded as 4500. The luminosity types I, II, III, IV, and V are coded as 1.5, 3.5, 5.5, 7.5, and 9.5, respectively. A F5V star is thus coded as 4509.5. In the present scheme, the luminosity class is given a low weight and the main emphasis on classification of the spectral types.

In the following we provide a discussion on the classification accuracy of the three sets of cases:

Cases A1-A3

The Cases A1-A3 use JHC as the training set with A1 and A2 in the wavelength region 4100-5500Å i.e. in the blue part of the spectrum. In the case A3, JHC was trained for the full span i.e. 3600-7400Å and tested on STELIB in the same band. The blue region classification error is lowest for ELODIE and somewhat inferior for CFLIB. However, the full

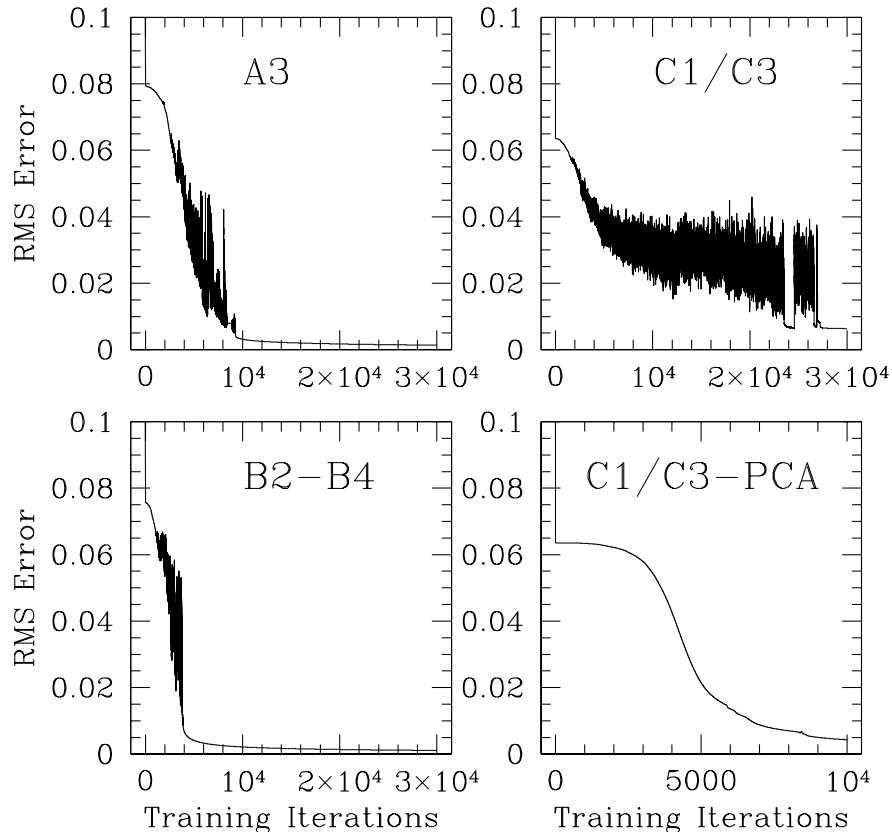


Fig. 4. ANN training session learning curves for some selected cases

span classification of STELIB deteriorates the error to about 861 i.e. 8.6 sub-spectral-type.

Cases B1-B4

In Case B1-B4, ELODIE was used as the training set and was tested on both ELODIE and CFLIB in the blue and full span. The training set of 174 spectra was preselected from amongst the 1959 ELODIE full set with one example spectra per spectro-luminosity class. The best classification is obtained for the case B1 with blue region of ELODIE. For the same region of CFLIB, i.e., case B2, the classification is somewhat inferior. The full span classification case B3 for ELODIE and case B4 for CFLIB are consequently with higher classification errors.

Cases C1-C3

Cases C1-C3 use STELIB as the training set and the test sets are CFLIB limited span C1; ELODIE limited span C3 and CFLIB full span case C2. The limited span cases of C1 and C3 show errors of 6.43 and 5.01 sub-spectral types but remarkably the case C2 with full span shows an error of only 6.7.

The most useful result as far as CFLIB is concerned, is the case C2 since the largest wavelength span is used for this case. It may be noted that except JHC, all other spectral

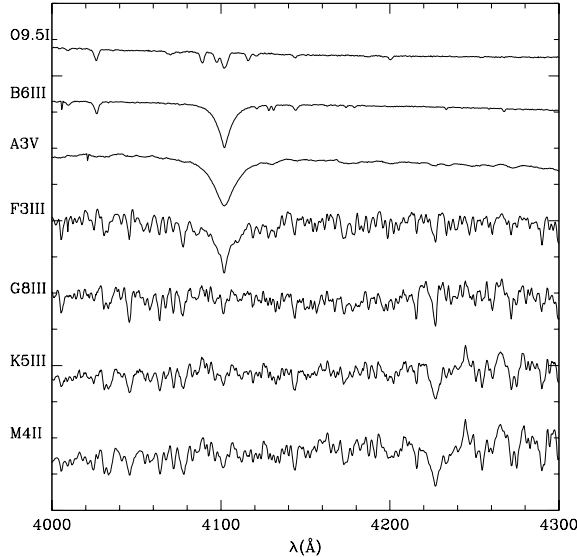


Fig. 5. Representative spectra of seven stars out of the total of 300 stars. The spectral types are listed on the vertical axis

libraries have gaps in them and this contributes greatly into the classification errors. Further, we also used a PCA based preprocessor for all the cases to reduce the dimensionality of the train-test sets as described in Singh et al. (1998). The resulting classification errors using first 15 principal components are only marginally poorer than the ones listed in the last column of Table 1. Last panel in Fig. 4 shows the scatter plot of case C1 with PCA.

Figure 4 displays some example learning curves of the ANN training sessions for Cases A3, B2-B4, C1-C3 and a PCA version of C1-C3. The B2-B4 (and C1-C3) are same training sessions. All the learning curves fall to a low rms learning error at the level on number of iterations of 30,000. The PCA version however requires much less number on iterations (~ 10000) to bring down these errors.

3. Restoration of Missing Data using PCA

To fill the gaps in the spectra one can use the data from a similar type star which doesn't have a gap at the same wavelength. However, we present here a preliminary study of an automated method for restoration of missing data for a set of spectra of 300 stars in the wavelength region 4000-4300 Å selected from the CFLIB. The list of stars with their spectral types is given in Table 3. The method of restoration is adopted from Unno and Yuasa (1992) and is briefly described here for the present data set.

To begin with, we have 301 flux values at 1 Å interval in the range for 4000-4300 Å for 300 stars. A sample of seven spectra are shown in Figure 5. For the i -th star, let F_j^i and w_j^i be the j -th observed flux value and its weight respectively, where $j = 1, \dots, n$ ($n = 301$) and $i =$

1,....., N (N = 300). If a particular flux value F_j^i for a particular star is missing, its weight is equal to zero.

For applying the PCA, the normalized data f_j^i is defined as

$$f_j^i = \frac{[F_j^i - \langle F_j \rangle]}{\sigma_j}, \quad (1)$$

where $\langle F_j \rangle$ and σ_j are the mean and the standard deviation of F_j respectively and are given by

$$\langle F_j \rangle = \frac{\sum_{i=1}^N w_j^i F_j^i}{\sum_{i=1}^N w_j^i}, \quad (2)$$

and

$$\sigma_j^2 = \frac{\sum_{i=1}^N w_j^i [F_j^i - \langle F_j \rangle]^2}{\sum_{i=1}^N w_j^i}. \quad (3)$$

Following Unno and Yuasa (1992), we define virtual data x_j^i and their corresponding weight v_j^i for each observed flux value f_j^i for each star as

$$v_j^i = 1 - w_j^i, \quad (4)$$

$$\sum_{i=1}^N v_j^i x_j^i = 0, \quad \sum_{i=1}^N v_j^i (x_j^i)^2 = \sum_{i=1}^N v_j^i. \quad (5)$$

Equation (5) represents the statistical constraint that the mean value of the virtual data is zero and the standard deviation is unity. For such a case, the correlation coefficient between the j-th quantity and the k-th quantity is defined by

$$C_{jk} = \frac{1}{N} \sum_{i=1}^N (w_j^i f_j^i + v_j^i x_j^i)(w_k^i f_k^i + v_k^i x_k^i). \quad (6)$$

The most probable value of x_j^i are thus given by the following set of n simultaneous linear algebraic equations:

$$\sum_{l=1}^n \frac{1}{\lambda_l} \left[\mu_{lj}^2 x_j^i + \sum_{k \neq j} \mu_{lj} \mu_{lk} (w_k^i f_k^i + v_k^i x_k^i) \right] = 0, \quad (j = 1, \dots, n), \quad (7)$$

where λ_l is the l -th eigenvalue and μ_l^j represent the j -th component of the l -th eigenvector in the PCA. The final adjusted value for the normalized j -th flux value for the i -th star is given by

$$w_j^i f_j^i + v_j^i x_j^i. \quad (8)$$

To check the veracity of this procedure let us assume that from the data set only one flux value F_1^s is missing. This means that $w_1^s = 0$ and all the other weights w_j^i except w_1^s are equal to unity. In this simplified situation, equations (7) reduce to

$$\left(\sum_{l=1}^n \frac{\mu_{l1}^2}{\lambda_l} \right) x_1^s + \sum_{l=1}^n \frac{\mu_{l1}}{\lambda_l} \left(\sum_{k=2}^n \mu_{lk} f_k^s \right) = 0, \quad (s = 1, \dots, N) \quad (9)$$

Table 2. Cases studied for flux restoration analysis using PCA

Case	Flux Reconst. at	No. of Principal Components	λ Region
(a)	4000 Å	10	4000-4009 Å
(b)	4077 Å	10	4077-4086 Å
(c)	4291 Å	10	4291-4300 Å
(d)	4000 Å	20	4000-4019 Å
(e)	4077 Å	20	4077-4096 Å
(f)	4281 Å	20	4281-4300 Å

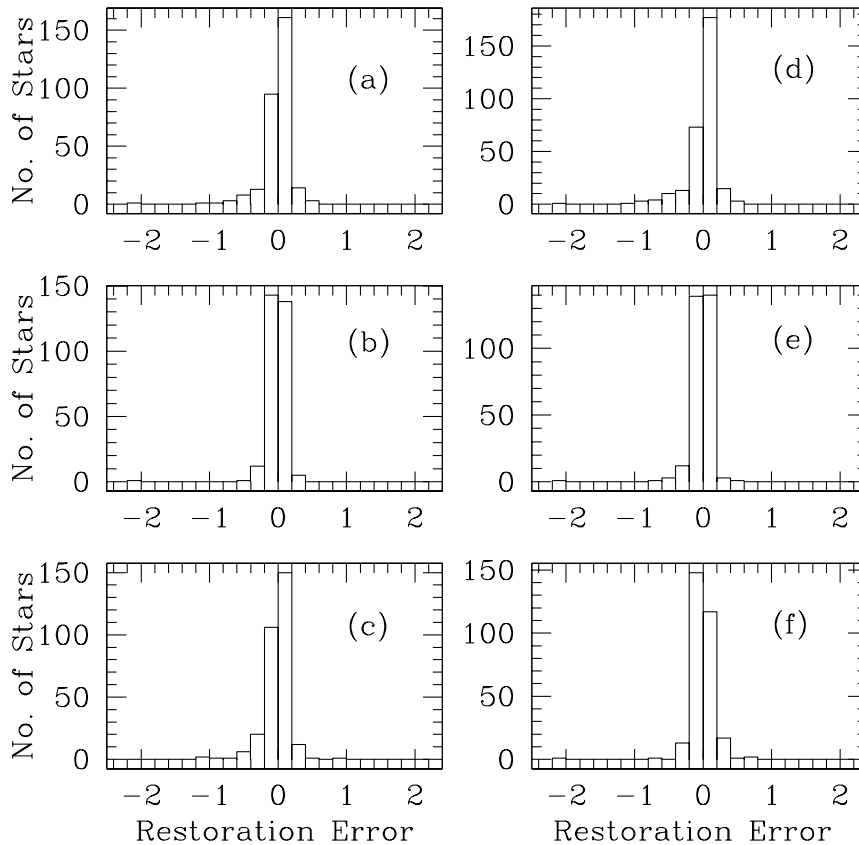


Fig. 6. Histogram of restoration error and the number of stars for the six cases. All stars with restoration errors greater than ± 0.2 are binned together

Equation (9) can be easily solved to get x_1^s for the missing flux f_1^s . By exchanging the columns, one can compute x_2^s , x_3^s , and so on for the missing flux for any wavelength and for any star. Six separate cases were studied and are listed in Table 2. The results of our preliminary analysis are shown in Figures 6 and 7.

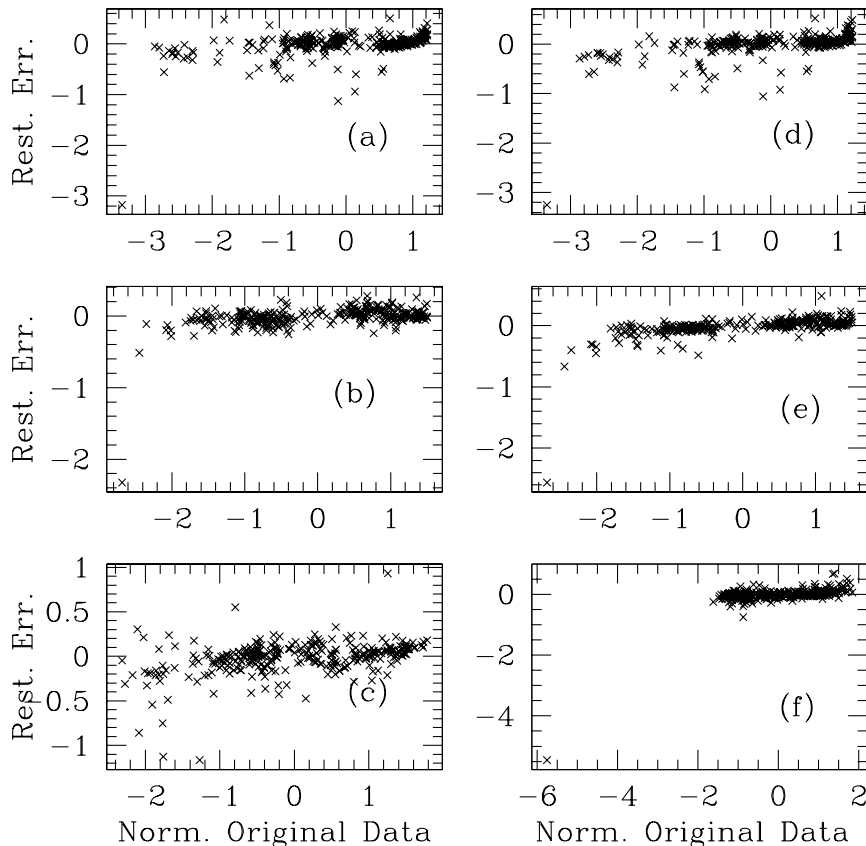


Fig. 7. Restoration error plotted against the normalized original data for all the six cases. The outlier at the bottom left of most of the plots is HD 31996

Case (a) uses a flux region of 10 \AA starting from 4000 \AA and thus 10 principal components to reconstruct the fluxes at 4000 \AA for all the 300 stars. From Fig. 6(a) we see that 256 stars have restoration error ($f_1^i - x_1^i$) within ± 0.1 . Fig. 7(a) shows the restored error vs. the original value of the normalized flux f_1^i (with mean zero). It is clear that for most of the stars the reconstruction is good. Case (d) uses 20 principal components and the reconstruction of flux at 4000 \AA is comparable, maybe slightly worse as is clear from Fig. 6(d) and Fig. 7(d).

We also tested the validity of this flux reconstruction method by attempting to reproduce a strong absorption feature, namely the 4077 \AA SrII feature, visible in the representative spectra in Fig. 5. Case (b) attempts to achieve this using 10 principal components rather successfully as is clear from Fig. 6(b) and Fig. 7(b) respectively. The flux at 4077 \AA was reconstructed to within ± 0.1 for a total of 281 stars out of 300. The case (e) with 20 principal components also reproduces the flux at 4077 \AA well although no better than case (b) (279 stars within ± 0.1) suggesting that the 10 PC's are enough for the data reconstruction in this data set. Lastly, cases (c) and (f) show similar behaviour in reconstructing towards the end of the wavelength interval and the results are plotted in Fig. 6(c and f) and Fig. 7 (c and f).

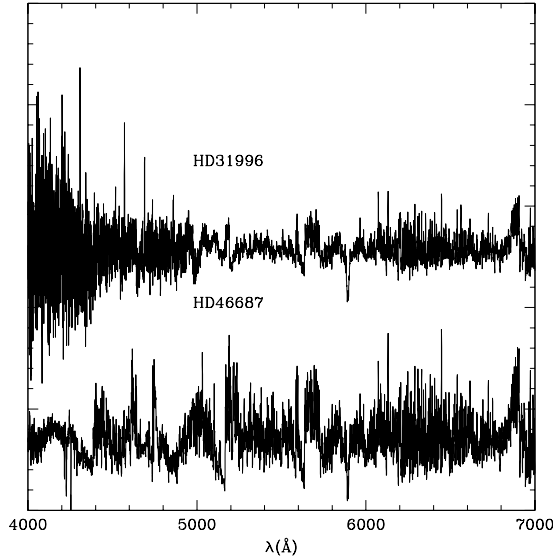


Fig. 8. Spectrum of the two stars HD 31996 and HD 46687 which have no known spectral types. Star HD 31996 is the outlier in the flux restoration analysis

Another interesting offshoot of this analysis was in picking outliers, stars which have either no known MK spectral types or have noisy spectra. Fig. 7(a,b,d,e,f) clearly show one outlier for which our scheme is unable to restore or reconstruct the fluxes. The star is HD 31996 and it indeed has no MK spectral class assigned to it (Table 3) as was verified from the CFLIB and the SIMBAD database. Another star, HD 46687, also has no known spectral type but its spectrum resembles a M type star. For this star, our analysis was able to reconstruct the fluxes. The spectra of these two stars obtained from the CFLIB are plotted in Fig. 8.

4. Conclusions

We have performed an extensive analysis based on artificial neural networks to classify stars in an automated manner in the Indo-US CFLIB using three databases viz., JHC, STELIB and ELODIE. The main aim of this exercise was two-fold. One was to perform the reliability checks on CFLIB to see how the gaps in the library affect the classification accuracy. We find that despite the presence of gaps, we have achieved classification accuracy of less than one main class. The second aim was to evolve and test automated procedures of classifying stellar spectra. This was achieved by trying our ANN scheme on ten different cases of training and testing on different pairs of libraries. The schemes are numerically intensive, with the ANN training stage requiring several hours of CPU time on the fastest of workstations. A PCA analysis was employed successfully to reduce the dimensionality of the data set and hence faster training without appreciable loss in classification accuracy.

Both STELIB and ELODIE libraries have variable spans of wavelength gaps where the

fluxes are filled with zeros (similar to CFLIB). Such gaps lead to classification errors in the PCA and ANN schemes. However, we have carried out some preliminary analysis with the basic χ^2 minimization scheme on these libraries wherein the gap portions were omitted in both train and test sets. This led to remarkable improvements in the classification accuracy.

We have also employed a generalized principal component analysis to first create and then fill the gaps in a sample of 300 stars out of the CFLIB in the blue region. At present, we have used a simplified system to reconstruct flux values at one wavelength bin at a time for these 300 stars. We hope to exploit the full potential of the scheme and attempt to fill larger gaps in stellar spectra in a subsequent study.

MY and HPS are grateful to JSPS (Japan Society for Promotion of Science) and DST (Department of Science & Technology, India) for financial support for exchange visits which made this work possible. MY would like to thank Emeritus Professor W. Unno of the University of Tokyo for helpful discussions. The research has made use of the SIMBAD database, operated by CDS, Strasbourg, France and the INDO-US CFLIB managed by NOAO, Tucson, AZ, USA.

Appendix 1. List of stars for data restoration analysis

The list of 300 stars with their HD numbers and the spectral types is given in Table 3. Two stars HD 31996 and HD 46687 have no known spectral types.

References

- Angel J. R. P., Wizinowich P., and Lloyd-Hart M. 1990, *Nature* 348, 221.
- Bailer-Jones C. A. L., Gupta R. and Singh H. P. 2002, in *Automated Data Analysis in Astronomy*, ed. R. Gupta, H. P. Singh and C. A. L. Bailer-Jones (Narosa, New Delhi) 51
- Le Borgne J.-F., Bruzual G., Pello, R., Lancon A., Rocca-Volmerange B., Sanahuja B., Schaerer D, Soubiran C. and Vilchez-Gomez R. 2003, *A&A* 402, 433L (STELIB)
- Cenarro A. J., Cardiel N., Gorgas J., Peletier R. F., Vazdekis A. and Prada F. 2001, *MNRAS* 326, 959
- Connolly A. J., Szalay A. S., Bershadsky M. A., Kinney L. A. and Calzetti D. 1995, *AJ* 110, 1071
- Folkes S. R., Lahav O. and Maddox S. J. 1996, *MNRAS* 283, 651
- Francis P. J., Hewett P. C., Foltz C. B. and Chaffee F. H. 1992, *ApJ* 398, 476
- Gupta R, Singh H. P., Volk K. and Kwok S. 2004, *ApJS* 152, 201
- Gulati R. K., Gupta R. and Rao, N. K. 1997, *A&A* 322, 933
- Gulati R. K., Gupta R. and Singh H. P. 1997, *PASP* 109, 843
- Jacoby G. H., Hunter D. A. and Christian C. A. 1984, *ApJS* 56, 257 (JHC)
- Johnston M. D. and Adorf H.-M. 1992, *Comput. Operations Res.* 19, 209
- Lahav O., Naim A., Sodr e L. Jr. and Storrie-Lombardi M. C. 1996, *MNRAS* 283, 207
- Moultaka J., Ilovaiski S.A., Prugniel P. and Soubiran C. 2004, *PASP* 116, 693 (ELODIE)
- Murtagh F. and Heck A. 1987, *Multivariate Data Analysis* (Reidel, Dordrecht)

Odehahn S. C., Stockwell E. B., Pennington R. L., Humphreys R. M. and zumach W. A. 1992, AJ 103, 318

Prugniel Ph. and Soubiran, C. 2001, A&A 369, 1048

Rumelhart D. E., Hinton G. E. and Williams R. J. 1986, Nature 323, 533

Singh H. P., Gulati R. K. and Gupta R. 1998, MNRAS 295, 312

Sodré L. Jr. and Cuevas H. 1994, Vistas Astron. 38, 331

Unno W. and Yuasa M. 1992, Ap&SS 189, 271

Unno W. and Yuasa M. 2000, PASJ 52, 127

Valdes F., Gupta R., Rose J. A., Singh, H. P. and Bell D. J. 2004, ApJS 152, 251 (CFLIB)

von Hippel T., Storrie-Lombardi L. J., Storrie-Lombardi M. C. and Irwin M. 1994, MNRAS 269, 97

Yuasa M., Unno W. and Magano S. 1999, PASJ 51, 197

Table 3. Sample of 300 stars used for data restoration analysis

HD No.	Sp. Type	HD No.	Sp. Type	HD No.	Sp. Type
100889	B9.5V	141680	G8III	191615	G8IV
102212	M1III	141714	G3.5III	195324	A1I
102224	K0.5III	142091	K1IV	196867	B9IV
102328	K3III	142198	K0III	198001	A1V
102870	F9V	142373	F8V	25329	K1V
103047	K0	143107	K2III	28978	A2V
103287	A0V	143666	G8III	29613	K0III
104985	G9III	143761	G0V	29645	G0V
105043	K2III	145328	K1III	30562	F8V
105262	B9	146791	G9.5III	30614	O9.5I
106365	K2III	147677	K0III	30652	F6V
106714	G8III	148387	G8III	30739	A1V
107113	F4V	148783	M6III	30743	F5V
107213	F8V	148786	K0III	30812	K1III
107383	G8III	149161	K4III	31295	A0V
107418	K0III	149630	B9V	31421	K2III
107950	G6III	149661	K2V	31996	0.0
108225	G9III	149757	O9V	32147	K3V
108954	F9V	150012	F5IV	33111	A3III
109317	K0III	150100	B9.5V	33256	F2V
109345	K0III	150117	B9V	35468	B2III
109358	G0V	150449	K1III	35497	B7III
110281	K5	150453	F3V	36673	F0I
110897	G0V	150680	G0IV	36861	O8III
111335	K5III	150997	G7.5III	37043	O9III
111591	K0III	151431	A3V	37160	K0III
111765	K4III	151613	F2V	37984	K1III
111812	G0III	151769	F7IV	38656	G8III
112300	M3III	151862	A1V	38899	B9IV
113226	G8III	152569	F0V	39003	G9.5III
113436	A3V	152614	B8V	39283	A2V
113848	F4V	152815	G8III	39587	G0V
113996	K5III	15318	B9III	39801	M1
114038	K1III	153597	F6V	39853	K5III
114092	K4III	153653	A7V	39866	A2II

Table 3. (Continued.)

HD No.	Sp. Type	HD No.	Sp. Type	HD No.	Sp. Type
114330	A1IV	153808	A0V	40035	K0III
114357	K3III	154278	K1III	40111	B0.5II
114642	F6V	154431	A5V	40136	F1V
114710	F9.5V	154445	B1V	40183	A2IV
115004	K0III	154660	A9V	40239	M3II
115136	K2III	155763	B6III	40536	A6
115202	K1III	157741	B9V	40801	K0II
115383	G0V	157910	G5III	41117	B2I
115539	G8III	158716	A1V	41330	G0V
115604	F3III	158899	K4III	41597	G8III
115617	G5V	159332	F6V	41636	G9III
116292	K0III	160765	A1V	41692	B5IV
116656	A2V	161056	B1.5V	42475	M1I
117176	G5V	161868	A0V	42543	M1I
117243	G5III	163588	K2III	43039	G8.5III
117818	K0III	163917	G9III	43042	F6V
117876	G8III	163989	F6IV	43232	K1.5III
118055	K0	164259	F2IV	43247	B9II
118266	K1III	164284	B2V	43318	F6V
120136	F6IV	164353	B5I	43380	K2III
120164	K0III	165029	A0V	43827	K1III
120348	K1III	165358	A2V	43947	F8V
120452	K0III	165401	G0V	44007	G5IV
121146	K2IV	165645	F0V	44033	K3I
121370	G0IV	165687	K0III	44478	M3III
122563	F8IV	165760	G8III	44537	M0I
123657	M4.5III	165908	F7V	44769	A5IV
123977	K0III	166014	B9.5V	44951	K3III
124570	F6IV	166046	A3V	45282	G0
124850	F7IV	166207	K0III	45410	K0III
124897	K1.5III	167042	K1III	45412	F8I
125451	F5IV	168151	F5V	46184	K1III
125454	G8III	168656	G8III	46687	0.0
126141	F5V	168723	K0III	47105	A0IV
126271	K4III	169191	K3III	47205	K1III

Table 3. (Continued.)

HD No.	Sp. Type	HD No.	Sp. Type	HD No.	Sp. Type
126868	G2IV	169414	K2III	47731	G5I
127334	G5V	170693	K1.5III	47839	O7V
128000	K5III	171301	B8IV	48329	G8I
128750	K2III	171391	G8III	48432	K0III
129312	G7III	172569	F0V	48433	K1III
129336	G8III	173087	B5V	48737	F5IV
129956	B9.5V	173399	G5IV	48781	K1III
129972	G8.5III	175317	F6IV	50420	A9III
129978	K2III	175535	G7III	51309	B3I
130948	G1V	175545	K2III	54662	O7III
131111	K0III	175588	M4II	54719	K2III
131156	G8V	175640	B9III	55280	K2III
132132	K1III	175743	K1III	55575	G0V
132345	K3III	175751	K2III	57264	G8III
133165	K0.5III	176301	B7III	57669	K0III
133208	G8III	176318	B7IV	57727	G8III
134083	F5V	176582	B5IV	58207	G9III
134190	G7.5III	176819	B2IV	58343	B2V
135742	B8V	177724	A0V	58551	F6V
136064	F9IV	177817	B7V	59881	F0III
136202	F8III	178125	B8III	60179	A1V
136512	K0III	178329	B3V	61064	F6III
136726	K4III	180006	G8III	61295	F6II
137052	F5IV	180711	G9III	62509	K0III
138716	K1IV	182293	K3IV	63302	K3I
139195	K0III	182568	B3IV	65714	G8III
139446	G8III	183144	B4III	65900	A1V
139641	G7.5III	184915	B0.5III	67228	G1IV
140027	G8III	188350	A0III	69897	F6V
141004	G0V	191243	B5I	70110	F9V